Clemens, S.C., Kuhnt, W., LeVay, L.J., and the Expedition 353 Scientists Proceedings of the International Ocean Discovery Program Volume 353 publications.iodp.org



https://doi.org/10.14379/iodp.proc.353.202.2020



Data report: revised late Miocene splice of IODP Site U1448 (353-U1448B-48F-1, 1 cm, to 353-U1448A-56X-5, 60 cm), Expedition 353, Indian Monsoon Rainfall¹

Janika Jöhnck², Wolfgang Kuhnt², and Ann Holbourn²

Keywords: International Ocean Discovery Program, IODP, JOIDES Resolution, Expedition 353, Indian Monsoon Rainfall, Site U1448, splice, X-ray fluorescence, late Miocene, composite depth

Contents

- **Abstract**
- Introduction
- 2 Material and methods
- Results and discussion
- Summary
- Acknowledgments
- References

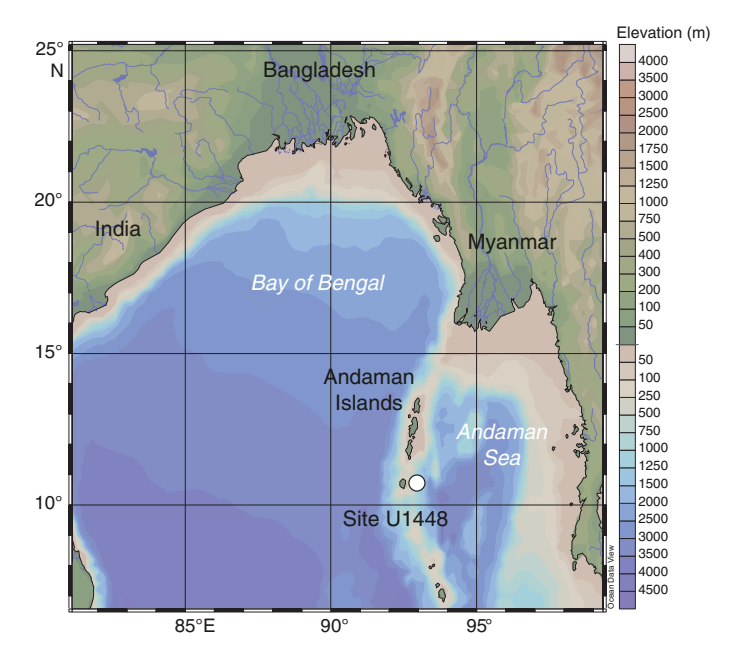
Abstract

We modified the original sediment splice of International Ocean Discovery Program (IODP) Expedition 353 Site U1448 over the interval 353-U1448B-48F-1, 1 cm, to 353-U1448A-56X-5, 60 cm, using new high-resolution X-ray fluorescence scanning data and linescan images. The revised splice now extends from 351.65 to 401.69 revised meters composite depth (r-mcd). We further appended the interval between 353-U1448A-53X-1, 0 cm, and 56X-5, 60 cm, thus extending the composite record down to 439.45 r-mcd.

Introduction

International Ocean Discovery Program (IODP) Expedition 353 targeted the reconstruction of Indian Monsoon precipitation and runoff variability in the Bay of Bengal since the late Miocene (Clemens et al., 2016b). Three holes were drilled at Site U1448 (10°38.03′N, 93°00.00′E; 1098 m water depth) in the Andaman Sea, ~44 km east of Little Andaman Island (Figure F1). The extended upper Pleistocene to upper Miocene succession consists of greenish gray hemipelagic clays with varying abundances of nannofossils, foraminifers, and biosiliceous components discordantly overlying middle Miocene greenish gray to light greenish gray biosiliceous oozes with varying proportions of clay and nannofossils. In Hole U1448A, Cores 1H-23H were drilled with the advanced piston corer (APC) system to 204.2 meters below seafloor (mbsf). Cores 24F-52F from 204.2 to 346.6 mbsf were recovered with the halflength APC (HLAPC) system. Hole U1448A was further deepened to 420.6 mbsf with the extended core barrel (XCB) drilling system, retrieving Cores 53X-60X. Hole U1448B was cored with the APC system from 0 to 177.71 mbsf (Cores 1H-19H) and with the HLAPC system from 179.2 to 358.22 mbsf (Cores 21F-58F). The late Miocene record ends with a hiatus at 379.11 mbsf in Section

Figure F1. Location of IODP Expedition 353 Site U1448 in the Bay of Bengal (white dot). Map generated with Ocean Data View (Schlitzer, 2015).



353-U1448A-65X-5, 60 cm, where upper Miocene sediments unconformably overlie lighter greenish gray middle Miocene biosiliceous ooze. Calcareous nannofossils and planktonic foraminifers in the core catcher sample above the hiatus indicate an age between 5.92 and 8.58 Ma, whereas the core catcher sample below the hiatus is older than 14.53 Ma (Clemens et al., 2016c).

A composite shipboard depth scale was originally constructed between 0 and ~260 meters composite depth (mcd) based on the

¹ Jöhnck, J., Kuhnt, W., and Holbourn, A., 2020. Data report: revised late Miocene splice of IODP Site U1448 (353-U1448B-48F-1, 1 cm, to 353-U1448A-56X-5, 60 cm), Expedition 353, Indian Monsoon Rainfall. In Clemens, S.C., Kuhnt, W., LeVay, L.J., and the Expedition 353 Scientists, Indian Monsoon Rainfall. Proceedings of the International Ocean Discovery Program, 353: College Station, TX (International Ocean Discovery Program). https://doi.org/10.14379/iodp.proc.353.202.2020

² Institute of Geosciences, Christian-Albrechts-University, Germany. Correspondence author: janika.joehnck@ifg.uni-kiel.de MS 353-202: Received 28 September 2019 · Accepted 6 February 2020 · Published 8 May 2020

magnetic susceptibility record obtained during Expedition 353 (Clemens et al., 2016a). The shipboard splice was revised between 0 and ~200 mcd using the SpliceFileFixer tool in the Correlator software (Stratigraphic correlation support [SCORS] applications are available at http://web.iodp.tamu.edu/apps) in March 2015 and extended to 411.38 mcd in January 2016 by S. Clemens (file available in the IODP Laboratory Information Management [LIMS] database: http://web.iodp.tamu.edu). This author used magnetic susceptibility between 0 and 17.97 mcd, color (red/green/blue green channel) between 17.97 and 136.48 mcd, and X-ray fluorescence (XRF)-scanner derived elemental ln(Ti/Ca) data between 136.48 and 411.38 mcd. Here, we present a revised splice based on XRF scanning data between 351.65 mcd and 401.69 revised meters composite depth (r-mcd) and extend this composite record to Section 353-U1448A-56X-5, 60 cm (439.45 r-mcd), by appending the interval between Sections 353-U1448A-53X-1, 0 cm, and 56X-5, 60 cm (see XRF in Supplementary material).

Material and methods

We performed XRF measurements at 1 cm intervals on the archive halves of Cores 353-U1448A-46F through 56X and 353-U1448B-48F through 58F using an Avaatech XRF core scanner at Kiel University (Germany). The instrument is equipped with an Oxford Instrument 50 W XTF5011 rhodium (Rh) X-ray tube and an Amptek XR-100CR detector. Prior to scanning, the core surface was scraped clean with a glass plate to obtain a fresh, smooth, and undisturbed surface without any contamination. The sediment surface was then covered with a Prolene thin film of 4 µm thickness to avoid pollution of the detector. All measurements were performed with an excitation window of 10 mm downcore and 10 mm crosscore slit size with a 10 s live counting time. We used a setting with a voltage of 10 kV and a current of 750 µA to detect the elements Al, Si, S, Cl, K, Ca, Ti, Cr, Mn, Fe, Co, Rb, Sr, and Rh and used the WIN AXIL Batch software for conversion of raw spectroscopic data to elemental counts. The XRF scanner data were then cleaned by removing unreliable measurements taken close to the plastic caps at the top and bottom of each section as well as measurements corresponding to small holes and core disturbances. To remove matrix effects, we calculated the logarithmic ratios of elemental counts that can be interpreted as relative concentrations (Weltje and Tjallingii, 2008) because it allows nondestructive extraction of near-continuous records of element intensities from sediment cores with a minimum of analytical effort. A disadvantage of XRF core scanning relative to conventional geochemical analysis is the problematic conversion of core-scanner output to element concentrations. The main reason for this long-standing problem is the poorly constrained measurement geometry, attributable to inhomogeneity of the specimens (e.g. variable water content and grain-size distribution). In this data report, we use the logarithmic ratio of iron and calcium (log[Fe/Ca]).

Results and discussion

The revised composite record between Cores 353-U1448B-48F and 353-U1448A-56X spans a length of 87.80 m. We used the intervals between Cores 353-U1448B-48F and 56F and between Cores 353-U1448A-46F and 56X. Our revised composite record consists of a 50.04 m long spliced interval between Cores 353-U1448B-48F and 353-U1448B-56F followed by a 36.26 m long sequence of cores from Hole U1448A, which was drilled with the XCB system down to

Table T1. Composite depth table for Cores 353-U1448B-48F to 353-U1448A-56X. **Download table in CSV format**.

the major hiatus at Section 353-U1448A-56X-5, 60 cm. We modified 6 tie points in the original splice based on correlation of XRF scanning $\log(\text{Fe/Ca})$ data and sedimentary features such as thin sandy layers identified in both Holes U1448A and U1448B. The changes in composite depth are expressed on a revised depth scale (r-mcd) (Table T1).

In the original splice, the base of Section 353-U1448A-46F-CC was tied directly to the top of Section 353-U1448B-50F-1. However, the log(Fe/Ca) records and linescan images revealed the presence of an unconformity at Section 353-U1448A-47F-1, 128 cm (364.30 rmcd) (Figure F2A). A further potential unconformity was visually identified at Section 353-U1448B-50F-1, 57 cm (365.86 r-mcd) (Figure F2B). We correlated the two sediment successions using a distinctive sandy layer that appears as a negative spike in log(Fe/Ca) at interval 353-U1448A-47F-2, 14-22 cm (364.58-364.66 r-mcd; 0.29 m below the unconformity in Hole U1448A), and at interval 353-U1448B-50F-2, 113-123 cm (367.68-367.78 r-mcd; 1.94 m below the unconformity in Hole U1448B) (Figure F2C, F2D). We appended Cores 353-U1448A-46F and 47F at 363.02 r-mcd and tied the last undisturbed sediments above the unconformity in Hole U1448A (47F-1, 127 cm; 364.29 r-mcd) to the first undisturbed sediments below the unconformity in Hole U1448B (50F-1, 64 cm; 365.79 r-mcd). Since the XRF scanning data indicate that the sediment record is not preserved in either hole, we inserted a gap of 1.5 m at this junction to compensate for missing material.

Between 379 and 397 r-mcd, we applied three minor adjustments to the original splice:

- 1. We removed ~5 cm of the splice at the tie point between Sections 353-U1448B-52F-3 and 353-U1448A-49F-1. We defined a more precise tie point at 379.79 r-mcd between Sections 353-U1448B-52F-3, 58 cm, and 353-U1448A-49F-1, 142 cm, by using a sandy layer (Figure F2E, F2F) expressed as a negative spike in both Holes U1448A and U1448B.
- Between 388 and 390 r-mcd, we removed Core 353-U1448B-54F from the splice because the XRF data indicate that this interval is likely disturbed and not in place, as shown by numerous outliers in the record from this core (Figure F2). As a new tie point, we appended Section 353-U1448A-51F-1 directly to Section 353-U1448A-50F-CC at 389.24 r-mcd.
- 3. We removed the upper ~1.7 m of Core 353-U1448B-55F from the original splice, thus eliminating duplication of a distinctive minimum in log(Fe/Ca). We defined a new tie point at 393.82 rmcd by correlating Sections 353-U1448A-51F-5, 66 cm, and 353-U1448B-55F-2, 26 cm (Figure **F2**).

In the original splice, Core 353-U1448A-52F was tied to Cores 353-U1448B-56F through 58F with the base of Section 353-U1448B-58F-CC marking the end of the splice. However, major discrepancies are evident when comparing the $\log(\text{Fe/Ca})$ records of Cores 353-U1448A-52F through 53X and 353-U1448B-56F through 58F (399–411 r-mcd; Figure F2). There are two maxima in $\log(\text{Fe/Ca})$ in Core 353-U1448B-56F, whereas only one maximum occurs at the intersection between Cores 353-U1448A-52F and 53X. Loss of sediment is likely at this level in Hole U1448A, due to the change from the HLAPC to XCB drilling technique. We therefore added a \sim 2 m interval from Core 353-U1448B-56F and defined a new tie point at 399.74 r-mcd at Sections 353-U1448A-52F-CC, 21 cm, and 353-U1448B-56F-2, 70 cm.

Figure F2. Site U1448 revised sediment splice, 351–371 r-mcd. XRF-derived log(Fe/Ca) plotted against revised mcd (r-mcd) in Hole U1448B (light blue, bottom panel), Hole U1448A (green, mid panel), and new composite record (top panel). Individual cores are labeled; length is indicated by brackets. Tie points are vertical lines in yellow (top tie point), red (bottom tie point), and red/yellow dashed (appended cores). Circled letters refer to the location of important sedimentary features; bracket length indicates length of interval shown. A. Interval 353-U1448A-47F-1, 120–142 cm (unconformity at 47F-1, 128 cm; 364.30 r-mcd). B. Interval 353-U1448B-50F-1, 46–68 cm (unconformity at 50F-1, 57 cm; 365.86 r-mcd). C. Interval 353-U1448A-47F-2, 0–22 cm (sandy layer at 47F-2, 14–22 cm; 364.58–364.66 r-mcd). D. Interval 353-U1448B-50F-2, 104–126 cm (sandy layer at 50F-2, 113–123 cm; 367.68-367.78 r-mcd). (Continued on next 3 pages.)

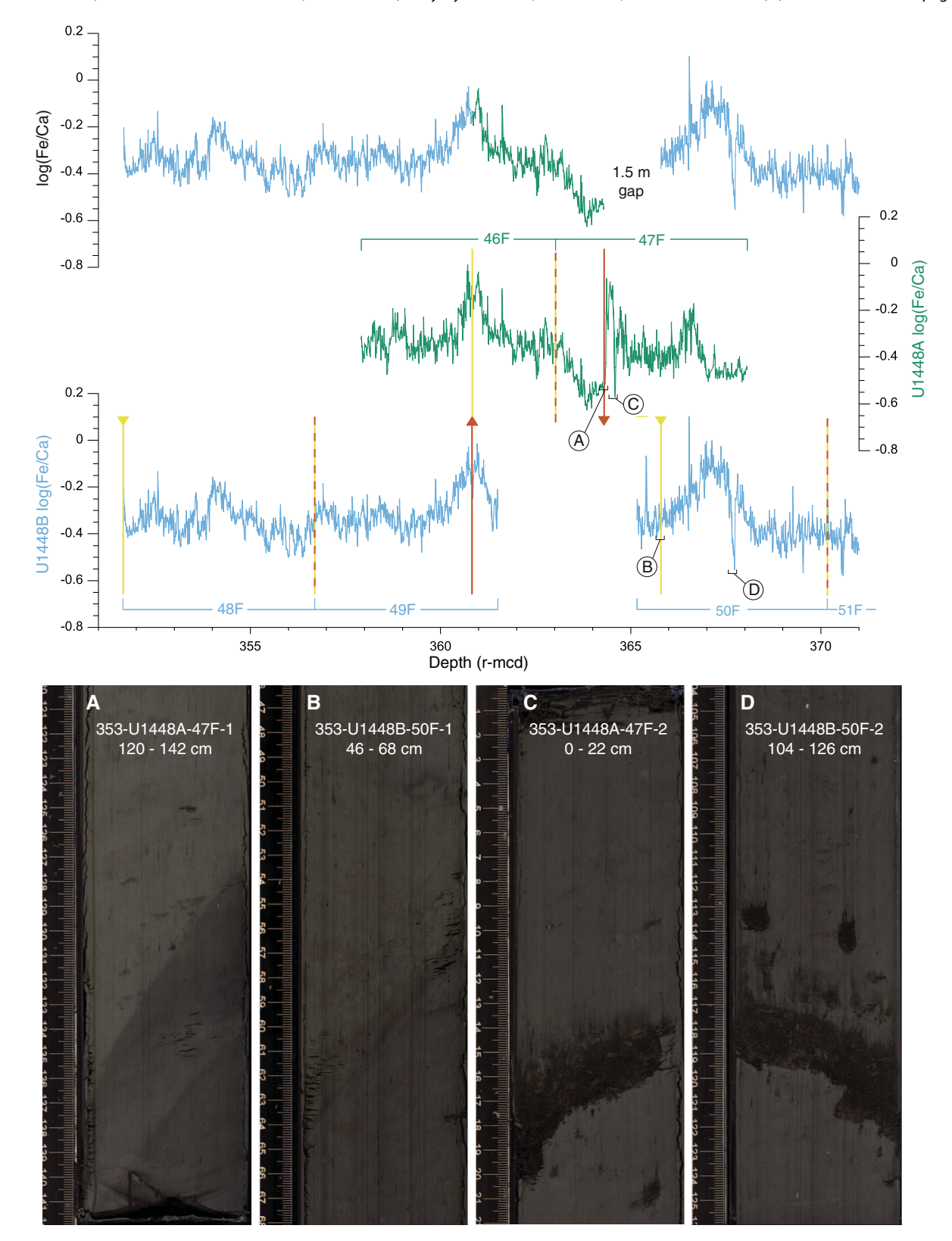
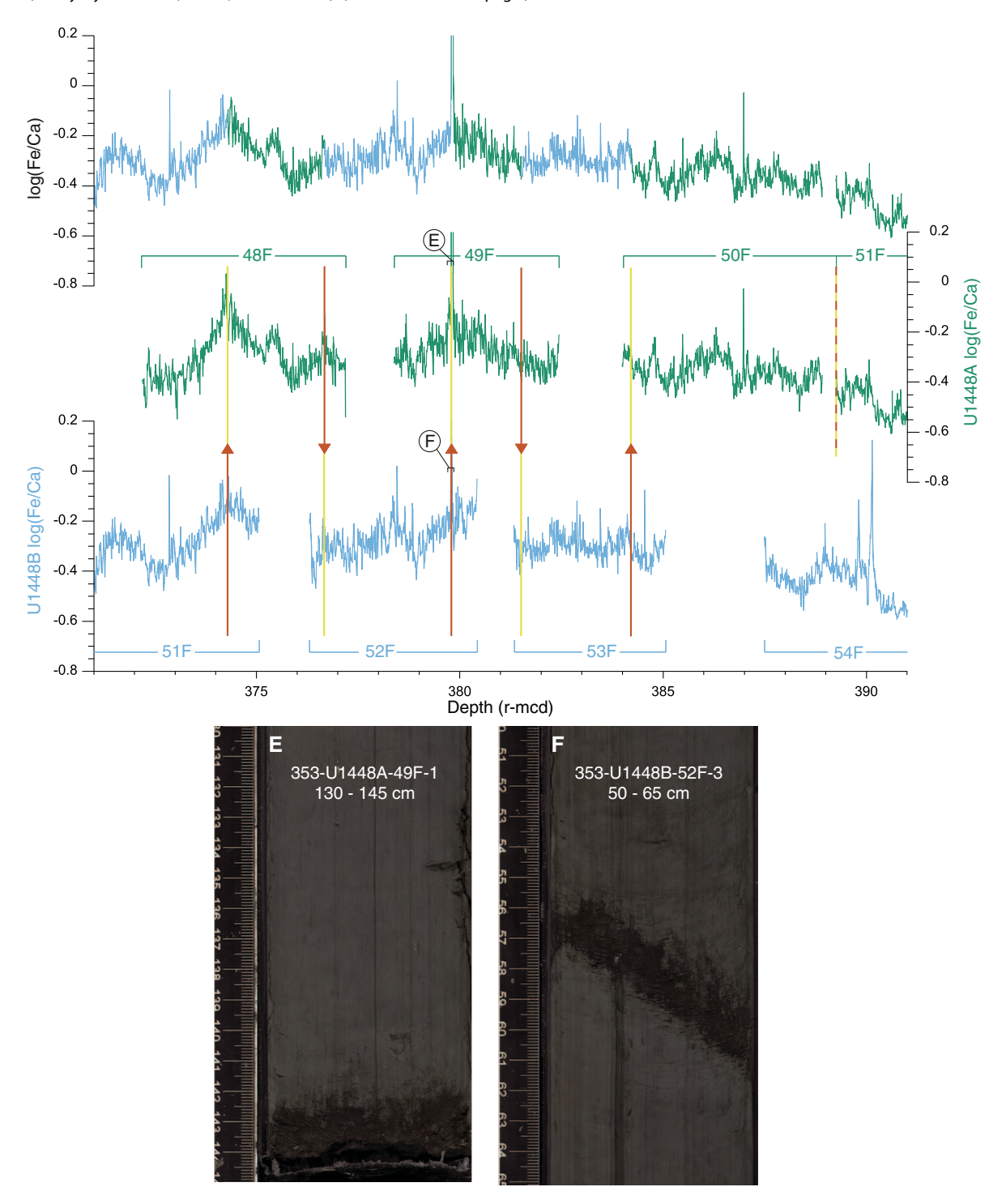


Figure F2 (continued). Site U1448 revised sediment splice, 371–391 r-mcd. Circled letters refer to the location of important sedimentary features; bracket length indicates length of interval shown. E. Interval 353-U1448A-49F-1, 130–145 cm (sandy layer at 49F-1, 142 cm; 379.79 r-mcd). F. Interval 353-U1448B-52F-3, 50–65 cm (Sandy layer at 52F-3, 58 cm; 379.79 r-mcd). (Continued on next page.)



We removed Cores 353-U1448B-57F through 58F from the splice because the interval between Sections 353-U1448B-57F-3, 0 cm, and 57F-4, 79 cm, appears disturbed due to vertical displacement of sediment (also detailed in the Site U1448 visual core descriptions) (Figure F2). Instead, we used the 36.26 m long interval from Section 353-U1448A-53X-1, 0 cm, to the hiatus at 65X-5, 60 cm, thus extending the splice to 439.45 r-mcd. We inserted a gap of 1.5 m at the tie point between Sections 353-U1448B-56F-CC, 4 cm

(401.69 r-mcd), and 353-U1448A-53X-1, 0 cm (403.19 r-mcd), to compensate for potential sediment loss during the change of coring equipment. A gap length of \sim 1.5 m would correspond to \sim 22 ky in the age domain. However, uncertainties remain regarding the extent of the core gap at this tie point because the record is not completely preserved in either hole. Cores 353-U1448A-53X through 56X-5, 60 cm, were appended without introducing any gaps between cores (Figure **F2**).

Figure F2 (continued). Site U1448 revised sediment splice, 391–411 r-mcd. (Continued on next page.)

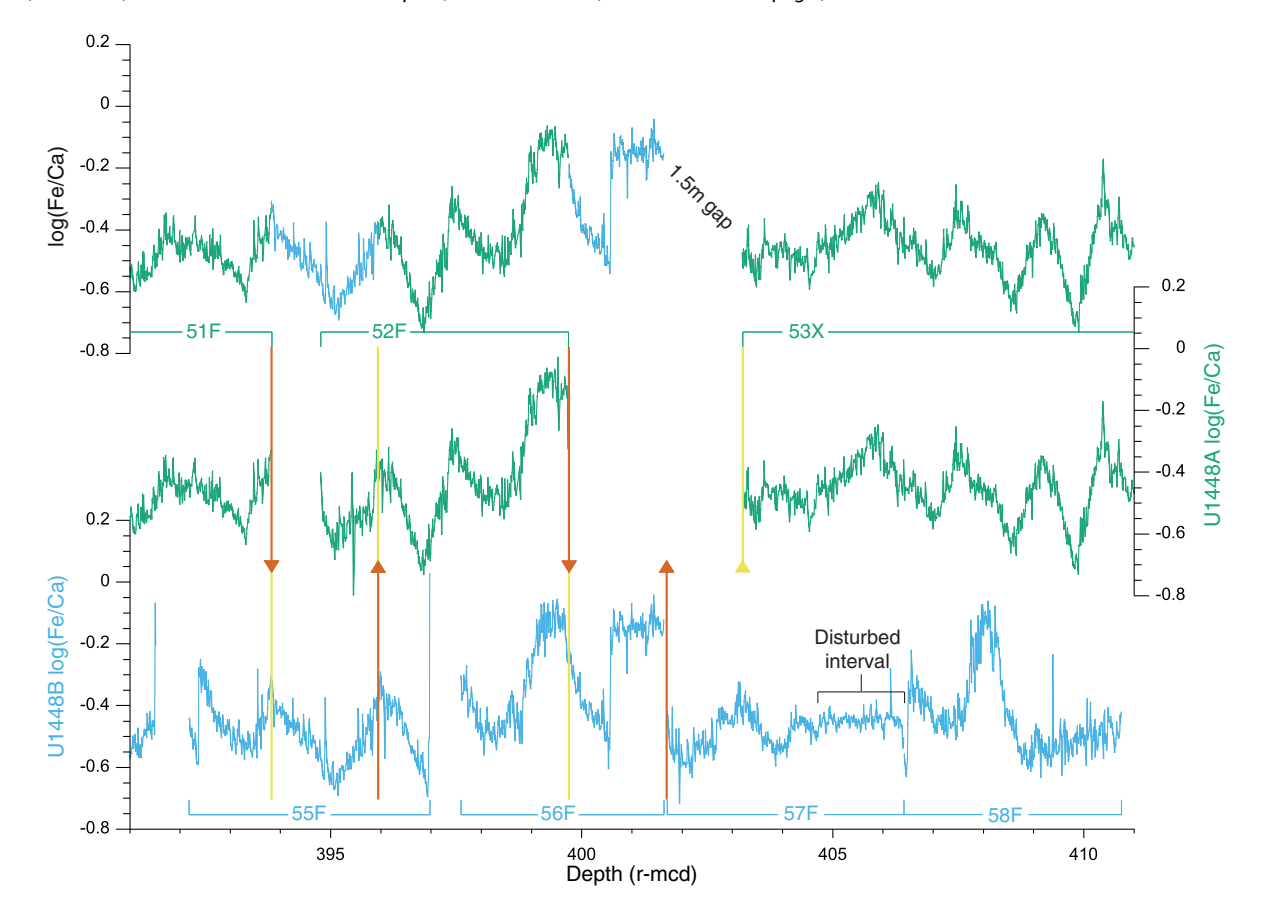
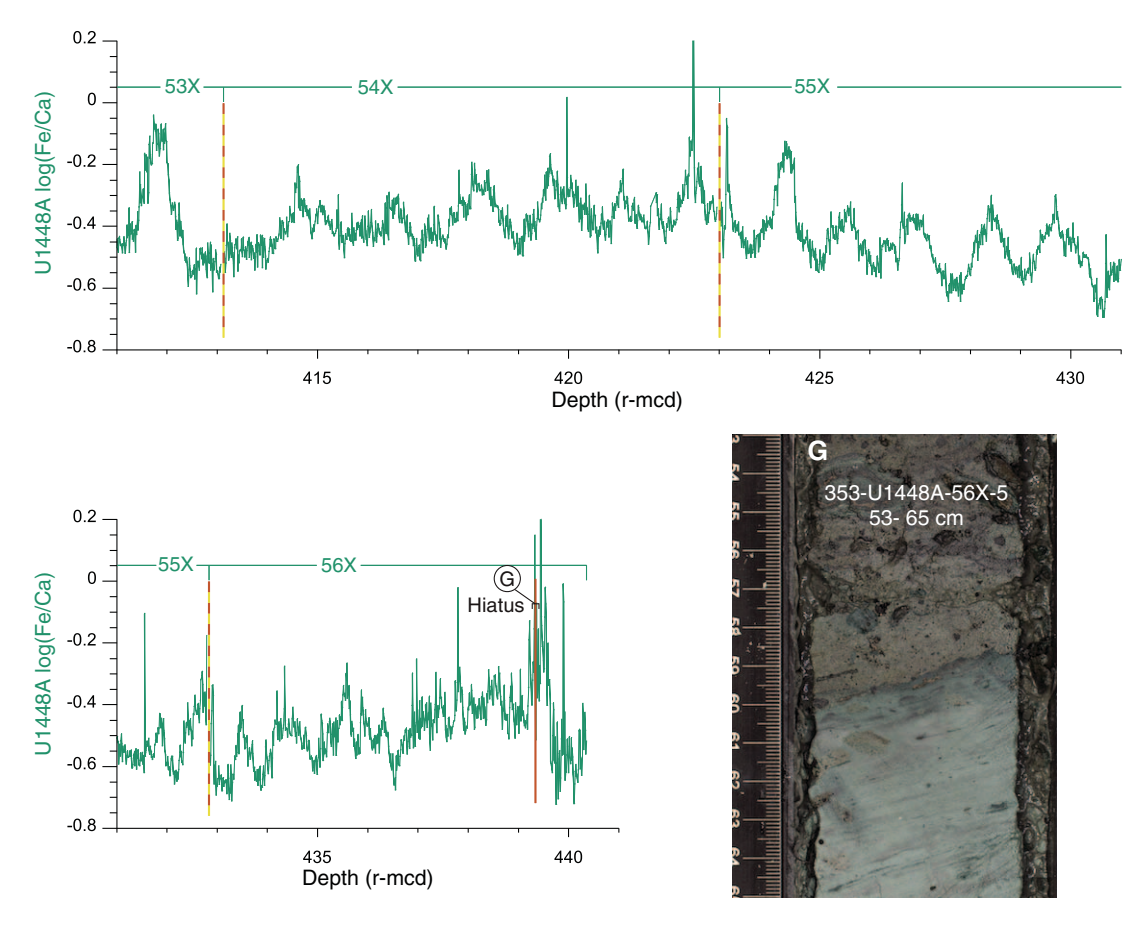


Figure F2 (continued). Site U1448 revised sediment splice, 411–431 r-mcd (top panel) and 431–441 r-mcd (lower panel), showing appended Cores U1448A-53X to 56X down to the hiatus at 439.45 r-mcd in Hole U1448A. Circled letter refers to the location of important sedimentary feature with bracket length indicating length of interval shown. G. Interval 353-U1448A-56X-5, 53–65 cm. Hiatus at 353-U1448A-56X-5, 60 cm (439.45 r-mcd).



Summary

We applied adjustments to the original late Miocene splice of Site U1448 by using new high-resolution X-ray fluorescence scanning data and linescan images. We present a revised composite record for the interval between Sections 353-U1448B-48F-1, 1 cm, and 353-U1448A-56X-5, 60 cm. We inserted small gaps to compensate for unconformities at the tie point between Sections 353-U1448A-47F-1 and 353-U1448B-50F-1 (1.5 m gap) and for the change in coring equipment during drilling of Core 353-U1448A-53X (1.5 m gap).

Acknowledgments

This research used samples and data provided by the International Ocean Discovery Program and was funded by the Deutsche Forschungsgemeinschaft. The postcruise XRF scanning at Kiel University was funded by the Deutsche Forschungsgemeinschaft (grant Ku649/35-1). We are most grateful to the Expedition 353 crew and Scientific Party, Ursula Röhl and the Bremen Core Repository staff for logistical assistance with the transport and storage of cores, and all XRF scanning helpers at Kiel University. We thank Sietske J. Batenburg for the helpful, constructive review.

References

Clemens, S.C., Kuhnt, W., LeVay, L.J., Anand, P., Ando, T., Bartol, M., Bolton, C.T., Ding, X., Gariboldi, K., Giosan, L., Hathorne, E.C., Huang, Y., Jaiswal, P., Kim, S., Kirkpatrick, J.B., Littler, K., Marino, G., Martinez, P., Naik, D., Peketi, A., Phillips, S.C., Robinson, M.M., Romero, O.E., Sagar, N., Taladay, K.B., Taylor, S.N., Thirumalai, K., Uramoto, G., Usui, Y., Wang, J., Yamamoto, M., and Zhou, L., 2016a. Expedition 353 methods. *In Clemens*, S.C., Kuhnt, W., LeVay, L.J., and the Expedition 353 Scientists, *Indian Monsoon Rainfall*. Proceedings of the International Ocean Discovery Program, 353: College Station, TX (International Ocean Discovery Program). https://doi.org/10.14379/iodp.proc.353.102.2016

Clemens, S.C., Kuhnt, W., LeVay, L.J., Anand, P., Ando, T., Bartol, M., Bolton, C.T., Ding, X., Gariboldi, K., Giosan, L., Hathorne, E.C., Huang, Y., Jaiswal, P., Kim, S., Kirkpatrick, J.B., Littler, K., Marino, G., Martinez, P., Naik, D., Peketi, A., Phillips, S.C., Robinson, M.M., Romero, O.E., Sagar, N., Taladay, K.B., Taylor, S.N., Thirumalai, K., Uramoto, G., Usui, Y., Wang, J., Yamamoto, M., and Zhou, L., 2016b. Expedition 353 summary. *In* Clemens, S.C., Kuhnt, W., LeVay, L.J., and the Expedition 353 Scientists, *Indian Monsoon Rainfall*. Proceedings of the International Ocean Discovery Program, 353: College Station, TX (International Ocean Discovery Program). https://doi.org/10.14379/iodp.proc.353.101.2016

Clemens, S.C., Kuhnt, W., LeVay, L.J., Anand, P., Ando, T., Bartol, M., Bolton, C.T., Ding, X., Gariboldi, K., Giosan, L., Hathorne, E.C., Huang, Y., Jaiswal, P., Kim, S., Kirkpatrick, J.B., Littler, K., Marino, G., Martinez, P.,

Naik, D., Peketi, A., Phillips, S.C., Robinson, M.M., Romero, O.E., Sagar, N., Taladay, K.B., Taylor, S.N., Thirumalai, K., Uramoto, G., Usui, Y., Wang, J., Yamamoto, M., and Zhou, L., 2016c. Site U1448. *In Clemens, S.C.*, Kuhnt, W., LeVay, L.J., and the Expedition 353 Scientists, *Indian Monsoon Rainfall*. Proceedings of the International Ocean Discovery Program, 353: College Station, TX (International Ocean Discovery Program). http://dx.doi.org/10.14379/iodp.proc.353.108.2016

Jöhnck, J., Kuhnt, W., and Holbourn, A., 2020. Supplementary material, https://doi.org/10.14379/iodp.proc.353.202supp.2020. Supplement to Jöhnck, J., Kuhnt, W., and Holbourn, A., 2020. Data report: revised late Miocene splice of IODP Site U1448 (353-U1448B-48F-1, 1 cm, to 353-U1448A-56X-5, 60 cm), Expedition 353, Indian Monsoon Rainfall. In Clemens, S.C., Kuhnt, W., LeVay, L.J., and the Expedition 353 Scientists, *Indian Monsoon Rainfall*. Proceedings of the International Ocean Discovery Program, 353: College Station, TX (International Ocean Discovery Program). https://doi.org/10.14379/iodp.proc.353.202.2020

Schlitzer, R., 2015. Data analysis and visualization with Ocean Data View. *CMOS Bulletin SCMO*, 43(1):9–13.

https://epic.awi.de/id/eprint/37570/

Weltje, G.J., and Tjallingii, R., 2008. Calibration of XRF core scanners for quantitative geochemical logging of sediment cores: theory and application. *Earth and Planetary Science Letters*, 274(3–4):423–438. https://doi.org/10.1016/j.epsl.2008.07.054